Published in final edited form as:
Synapse. 2010 April ; 64(4): 301–312. doi:10.1002/syn.20718.

Further evaluation of the carbon11-labelled $D_{2/3}$ agonist PET radiotracer PHNO: reproducibility in tracer characteristics and characterization of extrastriatal binding

Alice Egerton[1,2,3], **Ella Hirani**[4], **Rabia Ahmad**[4], **David R Turton**[5], **Diana Brickute**[5], **Lula Rosso**[3], **Oliver D Howes**[2,3], **Sajinder K Luthra**[4], and **Paul M Grasby**[1,3]

[1]Division of Neuroscience and Psychological Medicine, Department of Neuroscience and Mental Health, Imperial College London, London, W12 0NN, United Kingdom.

[2]Section of Neuroimaging, Institute of Psychiatry, King's College London, SE5 8AF, United Kingdom

[3]Medical Research Council Clinical Sciences Centre, Hammersmith Hospital, Du Cane Road, London W12 0NN, United Kingdom.

[4]MDX Research, GE Healthcare, Hammersmith Hospital, Du Cane Road, London W12 0NN, United Kingdom.

[5]Hammersmith Imanet Ltd, GE Healthcare, Hammersmith Hospital, Du Cane Road, London W12 0NN, United Kingdom.

Abstract

[^{11}C]-(+)-PHNO is a new dopamine $D_{2/3}$ receptor agonist radiotracer which has been successfully used to measure $D_{2/3}$ receptor availability in experimental animals and man. Here we report *in vivo* evaluation in the rat of the biodistribution, metabolism, specificity, selectivity and dopamine sensitivity of carbon-11 labeled PHNO ([^{11}C]-3-PHNO) produced by an alternative radiochemical synthesis method. [^{11}C]-3-PHNO showed rapid metabolism and clearance from most peripheral organs and tissues. [^{11}C]-3-PHNO, but not its polar metabolite, readily crossed the blood-brain barrier and showed high levels of uptake in the $D_{2/3}$ -rich striatum. Pre-treatment with unlabelled PHNO and the $D_{2/3}$ receptor antagonist raclopride indicated that binding in the striatum was specific and selective to $D_{2/3}$ receptors. PET studies in anaesthetized rats revealed significant reductions in [^{11}C]-3-PHNO binding in the striatum following amphetamine administration, indicating sensitivity to increases in endogenous dopamine concentrations. $D_{2/3}$ antagonist pre-treatment additionally indicated moderate levels of [^{11}C]-3-PHNO specific binding in several extrastriatal brain areas – most notably the olfactory bulbs and tubercles, thalamus and hypothalamus. Of particular interest, approximately 30% of [^{11}C]-3-PHNO signal in the cerebellum – a region often used as a 'low-binding' reference region for PET quantification - was attributable to specific signal. These data demonstrate that [^{11}C]-3-PHNO shows similar tracer characteristics to [^{11}C]-(+)-PHNO, but additionally indicate that radiolabeled PHNO may be used to estimate $D_{2/3}$ receptor availability in select extrastriatal brain regions with PET.

Corresponding Author: Dr Alice Egerton, Section of Neuroimaging, Institute of Psychiatry, King's College London, SE5 8AF, United Kingdom Alice.Egerton@iop.kcl.ac.uk**Tel:** +44 (0) 20 8383 3725 **Fax**: +44 (0) 20 8383 1783.

Europe PMC Funders Author Manuscripts

Keywords

PHNO; PET; dopamine; D2high; extrastriatal

Introduction

Positron emission tomography (PET) in combination with radiotracers that bind $D_{2/3}$ dopamine (DA) receptors may be used to measure $D_{2/3}$ receptor availability and changes in extracellular DA concentrations in the living brain. Whilst conventional $D_{2/3}$ radiotracers are antagonists, recent years have seen considerable efforts to develop and optimize $D_{2/3}$ agonist radiotracers for PET imaging. $D_{2/3}$ agonist radiotracers are desirable for two theoretical reasons: they may afford greater sensitivity in detecting changes in extracellular DA than antagonist compounds, and they may allow specific investigation of changes in D_2 receptor agonist binding capacity in neuropsychiatric disorders.

Alterations in the extent of DA release may underlie the pathophysiology of several neuropsychiatric disorders. Through competition with DA for $D_{2/3}$ receptor binding, PET radiotracers may index changes in DA levels; decreases in radiotracer binding potentials (BPs) are interpreted as increases in DA release. Whilst the ability of $D_{2/3}$ antagonist radiotracers to measure changes in extracellular DA levels is well established, the magnitude of BP change following experimental manipulations is small, reaching a ceiling effect of ~40% (Laruelle, 2000). Increased sensitivity of $D_{2/3}$ radiotracers in detecting changes in DA concentrations is therefore highly desirable.

D_2 receptors exist in intraconvertible high (D_2^{high}) and low (D_2^{low}) affinity states for agonist binding; the D_2^{high} state is regarded as the functional state due to G-protein coupling (Sibley et al. 1982). The endogenous agonist DA has an *in vitro* affinity of 1-10nM for receptors in the D_2^{high} conformation; this D_2^{high} affinity is ~100-fold higher than affinity at D_2^{low} sites (around 0.7-1.5 μM) (Freedman et al. 1994; Richfield et al. 1989; Seeman et al. 2003; Sibley et al. 1982; Sokoloff et al. 1990; Sokoloff et al. 1992). Theoretically, D_2 agonist radiotracers should have greater sensitivity than D_2 antagonist radiotracers in detecting changes in endogenous DA levels as, at tracer doses, competition between DA and the radiotracer should occur predominantly at D_2^{high} sites (Cumming et al., 2002; Hwang et al., 2005; McCormick et al., 2008; Narendran et al., 2004; Seneca et al., 2006; Wilson et al., 2005;). In addition, affinity at the D_3 receptor may also increase radiotracer DA sensitivity, as DA has approximately 20-fold selectivity for D_3 over D_2 sites (Freedman et al., 1994; Narendran et al., 2006; Sautel et al., 1995; Sokoloff et al., 1990). Furthermore, alterations in the proportion of D_2 receptors in the high affinity state may contribute to neuropsychiatric pathophysiology (Seeman et al., 2005a; 2006). Availability of $D_{2/3}$ agonist radiotracers will theoretically allow measurement of D_2^{high} *in vivo* in human clinical populations (Ginovart et al., 2007; Graff-Guerrero et al., 2008a,b; Willeit et al., 2006; 2008).

Several $D_{2/3}$ agonist radiotracers have recently been developed, including the apomorphine derivative (−)-N-[^{11}C]propyl-norapomorphine ([^{11}C](−)-NPA) (Hwang et al., 2000) and the napthoxazine [^{11}C]-(+)-PHNO ([^{11}C](+)-4-propyl-3,4,4a,5,6,10b-hexahydro-2H-naphtho[1,2-b][1,4]oxazin-9-ol) (Wilson et al., 2005). *In vitro*, PHNO has over 100-fold

Europe PMC Funders Author Manuscripts

selectivity for D_2^{high} over D_2^{low} sites, the K_i at cloned human D_2^{high} receptors is ~0.24nM (Madras et al., 1988; Seeman and Ulpian, 1988; Seeman et al., 1993; Seeman et al., 2005b). PHNO also has affinity at the D_3 receptor subtype (total D_3 population, K_i = 0.16nM; D_3^{high}, K_i = 0.6nM) (Freedman et al., 1994; Seeman et al., 2005b), which may account for a large proportion of the [^{11}C]-(+)-PHNO specific binding signal *in vivo* (Narendran et al., 2006; Rabiner et al., 2009).

[^{11}C]-(+)-PHNO was first synthesized at the MRC Cyclotron Unit in 1997 (Brown et al., 1997) and has since been developed and characterized as a PET radiotracer by Wilson and colleagues at the Centre for Addiction and Mental Health (CAMH), University of Toronto, Canada (Wilson et al., 2005). Several studies in rat, cat and baboon show that [^{11}C]-(+)-PHNO demonstrates an excellent $D_{2/3}$ radiotracer profile (Galineau et al., 2006; Ginovart et al., 2006; McCormick et al., 2008; Narendran et al., 2006; Rabiner et al., 2009; Wilson et al., 2005). [^{11}C]-(+)-PHNO brain uptake is rapid and the regional distribution is accordant with $D_{2/3}$ receptor expression, and binding is saturable and selective for $D_{2/3}$ receptors. [^{11}C]-(+)-PHNO binding in the striatum is sensitive to pharmacological manipulations that increase (RTI-32, amphetamine) or decrease (AMPT, reserpine) endogenous DA levels. This DA sensitivity to amphetamine is greater than that of the $D_{2/3}$ antagonist radiotracer [^{11}C]raclopride, at least under some experimental conditions (Galineau et al., 2006; Ginovart et al., 2006; McCormick et al., 2008; Narendran et al., 2006; Willeit et al., 2007).

The regional distribution of [^{11}C]-(+)-PHNO in the human brain parallels that observed in experimental animals (Ginovart et al., 2007; Graff-Guerrero et al., 2008a;b; Willeit et al., 2006; 2008). In the human striatum, [^{11}C]-(+)-PHNO binding is $D_{2/3}$ receptor-specific (Willeit et al., 2006), and sensitive to increases in DA concentrations elicited by amphetamine administration (Willeit et al., 2008). Kinetic modeling of [^{11}C]-(+)-PHNO in man indicates that regional brain uptake can be described by standard kinetic models and the cerebellum may be acceptable for use as a reference region in determination of regional [^{11}C]-(+)-PHNO BP, thus avoiding the requirement for arterial cannulation and blood sampling (Ginovart et al., 2007).

As the above studies indicated that [^{11}C]-(+)-PHNO shows great promise as a $D_{2/3}$ agonist PET tracer, we wished to confirm and extend preclinical characterization of [^{11}C]-(+)-PHNO. In an attempt to simplify and improve the radiochemical labeling of [^{11}C]-(+)-PHNO, an alternative radiochemical synthesis method was employed which resulted in ^{11}C labeling at a different molecular position ([^{11}C]-3-PHNO). The aims of the current study were to determine, *ex vivo*, in rats whether [^{11}C]-3-PHNO shows an equivalent profile of metabolism, brain uptake and kinetics, biodistribution and $D_{2/3}$ receptor binding specificity to that previously published for [^{11}C]-(+)-PHNO (Galineau et al., 2006; Ginovart et al., 2006; McCormick et al., 2008; Narendran et al., 2006; Rabiner et al., 2009; Wilson et al., 2005). In addition, we investigated the sensitivity of [^{11}C]-3-PHNO to amphetamine-induced increases in DA concentrations elicited by amphetamine administration using PET in anaesthetized rats.

Materials and Methods

Radiochemistry

The previously published method for [^{11}C]-(+)-PHNO synthesis uses an [^{11}C]-acid chloride synthesis route (Brown et al., 1997; Wilson et al., 2005). With the aim of improving the reliability of radiochemical synthesis, a novel route for [^{11}C]-(+)-PHNO synthesis was developed (García-Argüello, 2007). In comparison to the previously published [^{11}C]-(+)-PHNO synthesis method (Wilson et al., 2005), the novel route employed here resulted in [^{11}C]-labeling at the terminal carbon of the *N*-propyl chain (Figure 1). We term the radiolabeled PHNO used in the present investigations [^{11}C]-3-PHNO ((+)-4-(3-[^{11}C]-propyl)-3,4,4a,5,6,10b-Hexahydro-2H-Naphtho[1,2-b][1,4]Oxazin-9-ol)), in order to discriminate it from that previously published ((+)-4-(1-[^{11}C]-propyl)-3,4,4a,5,6,10b-hexahydro-2H-naphtho[1,2-b][1,4]oxazin-9-ol) (Wilson et al., 2005). At the time of the biological investigations detailed here, this radiosynthesis method was at the development stage and radiochemical yields of [^{11}C]-3-PHNO suitable for preclinical use were reliably achieved. The specific activity at time of injection was 50.58±23.77 GBq/μmol (range 26.80 to 81.05 GBq/μmol), with an associated co-injected stable PHNO content of 0.89±0.34 nmol/kg. At this stage, reliability of [^{11}C]-3-PHNO radiosynthesis was similar to that reported for [^{11}C]-(+)-PHNO; Wilson et al., (2005) report 33-67 GBq/μmol [^{11}C]-(+)-PHNO specific activity at the end of radiochemical synthesis reported and Galineau et al., (2006) report 31-76 GBq/μmol specific activity at time of injection.

Animals

A total of 31 adult male Sprague–Dawley rats (Harlan Olac, UK) (body weight mean ± S.D. = 283 ± 19g) were group housed in standard conditions. All investigations were carried out in accordance with the UK Animals (Scientific Procedures) Act, 1986 and associated guidelines. In all cases, rats were prepared for intravenous injection of [^{11}C]-3-PHNO by surgically catheterizing the tail vein under anesthesia. In cases where [^{11}C]-3-PHNO was administered to non-anesthetized rats, animals were allowed to recover under light restraint in Bollman cages for ~2 hours prior to [^{11}C]-3-PHNO administration.

In vivo biodistribution

The temporal pattern of biodistribution of [^{11}C]-3-PHNO across selected brain regions and peripheral tissues was determined in 12 non-anesthetized rats. Each rat was injected with ~280 μCi [^{11}C]-3-PHNO i.v. and 2, 10, 30 or 60 minutes later animals were euthanized via an intravenous injection of sodium pentobarbitone (3 animals at each time point). Brains were rapidly removed and 13 brain regions were dissected out (striatum, olfactory bulbs, olfactory tubercles, hypothalamus, thalamus, prefrontal cortex, somatosensory cortex, entorhinal cortex, hippocampus, inferior colliculi, superior colliculi, medulla with pons, cerebellum). These brain regions represent samples with a range of $D_{2/3}$ receptor densities. 17 peripheral tissues and fluids were collected (heart, lung, liver, kidney, spleen, stomach, duodenum, duodenum content, large intestine, large intestine content, testis, skeletal muscle, fat, skin, urine, with whole blood and plasma obtained from samples collected from the ventricle, post-mortem). Samples were added to pre-weighed vials and radioactivity was measured using a Wallac gamma-counter, with automatic correction for radioactive decay.

The radioactivity in tissue samples is expressed as 'uptake units': the percentage of the injected dose per gram of wet tissue weight, normalized to body weight, giving:

$$\text{uptake units} = (\text{cpm/g tissue}) / (\text{injected cpm/g body weight})$$

.

Here, uptake units represent free, non-specifically and specifically bound radiotracer. Specific binding of [^{11}C]-3-PHNO in individual brain regions was calculated as the specific binding ratio (SBR), estimated as the ratio of total uptake in a region of interest (ROI) to total uptake in the cerebellar reference tissue, as representative of the non displaceable (free plus non specific) binding uptake:

$$SBR = \left(\text{uptake units}_{(\text{tissue})} - \text{uptake units}_{(\text{cerebellum})}\right) / \text{uptake units}_{(\text{cerebellum})}$$

This approach assumes that the reference tissue (cerebellum) has a negligible number of receptors to which the radiotracer in question will specifically bind and that the non-specifically bound radiotracer shows similar behavior in the brain region of interest and the reference region (Hume et al., 1992). As the cerebellum has low D_2 receptor binding (Camps et al., 1990; Levant et al., 1993), this region is commonly used as a reference tissue for data obtained using D_2 radiotracers, and has been used for quantification of [^{11}C]-(+)-PHNO specific binding in several species (Galineau et al., 2006; Ginovart et al., 2006; 2007; Graff-Guerrero et al., 2008a;b; McCormick et al., 2008; Narendran et al., 2006; Rabiner et al., 2009; Willeit et al., 2006; 2008; Wilson et al., 2005).

Competition studies

Awake rats were intravenously administered a saturating dose of either unlabelled PHNO (1 mg/kg; n = 4), or the $D_{2/3}$ antagonist raclopride (2 mg/kg; n = 4). Five minutes later, each rat was injected with ~280μCi [^{11}C]-3-PHNO. 60 minutes following [^{11}C]-3-PHNO administration, animals were euthanized via an intravenous injection of sodium pentobarbitone. Radioactivity was measured in 12 brain regions of interest and expressed as uptake units as detailed above. Regional specific binding of [^{11}C]-3-PHNO was determined by comparison of regional [^{11}C]-3-PHNO uptake units following unlabelled PHNO or raclopride with data obtained in 3 control animals (no pre-treatment) at the same 60 minute time-point.

Metabolism

The presence of radiolabeled [^{11}C]-3-PHNO metabolites in the plasma and brain was measured in 3 animals. Awake rats were administered ~320μCi [^{11}C]-3-PHNO i.v. At 2, 10, 20, 30 or 60 minutes, blood samples were collected via a tail arterial catheter. Animals were euthanized via an intravenous injection of sodium pentobarbitone 10, 30 or 60 minutes after [^{11}C]-3-PHNO administration and the cerebrum was excised. Both brain and plasma samples were immediately de-proteinated. Plasma samples were added to ice-cold acetonitrile (1:10 v/v; plasma:acetonitrile) and centrifuged at 13,000g for 3 minutes. Brain

tissue was added to 10mls of ice-cold acetonitrile and homogenised using a polytron homogenizer set at half-maximum speed for 1-2 minutes. The resulting plasma and brain supernatants were concentrated by rotary evaporation and the residues were re-suspended in 2.5mls of mobile phase. Samples were filtered and 1ml of the ultrafiltrate was injected onto the HPLC column.

Metabolite analysis of plasma and brain tissue was determined on a reverse-phase C18 μ-Bondapak HPLC column (300 × 7.8mm;10μm) using a mobile phase of acetonitrile and 0.1M ammonium formate (30:70 v/v) at a flow rate of 3ml/min with ultraviolet absorbance at 210nm and radiochemical detection. The detectors were connected to a PC based electronic integration system, which allowed for the percentage of each radiolabeled component to be calculated (LauraLite software, Lablogic Ltd.).

Positron emission tomography

PET imaging in anesthetized rats was used to visualize the brain distribution of [^{11}C]-3-PHNO *in vivo* and to determine the sensitivity of [^{11}C]-3-PHNO to increases in extracellular DA concentrations elicited by amphetamine administration. Anesthetized rats were administered either vehicle (0.9% NaCl, n = 6) or 4mg/kg amphetamine sulphate (Sigma UK, n = 5) i.p. 30 minutes prior to [^{11}C]-3-PHNO injection. To ensure correct head position, rats were positioned in a stereotaxic frame (made in-house) and placed in a quad-HIDAC (high-density avalanche chamber) small animal tomograph (Oxford Positron Systems). Immediately following i.v. administration of ~280μCi [^{11}C]-3-PHNO, emission data were acquired in list mode for 60 minutes. At the end of the scan, rats were euthanized via an intravenous injection of sodium pentobarbitone. Brain tissue was dissected from vehicle-treated control rats and processed as above for analysis of radiotracer uptake in brain ROI.

To reconstruct scan sinograms, list mode emission data were binned into 0.5mm isotropic voxels using filtered back-projection (Hamming filter, 0.6 cut-off). This resulted in a spatial resolution of ~0.5mm full width at half-maximum (FWHM) (Myers and Hume, 2002). Image volumes were then transferred into ANALYZE software for volume of interest (VOI) analysis (Robb, 2001). To sample [^{11}C]-3-PHNO binding, a VOI template based on stereotaxic coordinates (Hume et al., 2001) was projected onto each scan volume. Data were sampled from the dorsal striatum (2 × 140 voxels), ventral striatum (2 × 32 voxels) and cerebellum (784 voxels). We also sampled data in VOIs placed in several extrastriatal regions in which moderate levels of radiolabeled PHNO specific binding have been indicated either by the biodistribution data in the present study or previously published data (Narendran et al., 2006; Nobrega and Seeman, 1994; Rabiner et al., 2009; Willeit et al., 2008). These regions included the olfactory tubercles and olfactory bulbs, thalamus, hypothalamus, globus pallidus, substantia nigra / ventral tegmental area, pons and medulla, inferior and superior colliculi, hippocampus and frontal and somatosensory cortices.

The total binding: non specific binding ratio in each VOI was calculated from tissue: cerebellum ratios. Although data from the quad-HIDAC scanner was in list-mode, allowing rebinning into dynamic time-activity curves, the low sensitivity of the scanner and thus low count statistics do not allow measurement of tissue concentrations in VOI with low signals such as the cerebellum (Hirani et al., 2003; Hume et al., 2001). To increase count statistics,

data analysis was limited to calculation of the SBR ((VOI-cerebellum)/cerebellum) during to a single 40 minute time-frame, beginning 20 minutes after [^{11}C]-3-PHNO injection. This approach assumes pseudo-equilibrium from 20-60 minutes after [^{11}C]-3-PHNO injection. The biodistribution study indicates that pseudo-equilibrium is established in this time period. This approach is further supported by a study of [^{11}C]raclopride showing that ratio data acquired in the 20-60 minute time frame correlates well with individual binding potential measurements derived from time-activity curves (Houston et al., 2004).

Statistical analysis

All data were checked for homogeneity of variance. For competition studies, group effects were determined using one-way analysis of variance in each of the 12 ROIs. For PET data, the effects of amphetamine administration versus control on dorsal and ventral striatal [^{11}C]-3-PHNO SBR were determined using 2-tailed independent sample t-tests. In all cases the threshold for statistical significance was set at an alpha-level of 0.05 and statistical analysis was performed using SPSS software for Windows (SPSS Inc. Version 16.0).

Results

Biodistribution of [^{11}C]-3-PHNO in peripheral organs and tissues

Table 1 presents data relating to the time-course of ^{11}C radioactivity distribution in peripheral organs and tissues following [^{11}C]-3-PHNO administration. At the earliest time-point (2 minutes) the highest levels of radioactivity were recorded in the lung, kidney and content of the small intestine. Skeletal muscle, fat, skin, large intestine content and urine showed low levels of initial radioactivity uptake. In most organs initial uptake was followed by rapid clearance and accumulation of radioactivity did not occur in any of the organs or tissues analyzed. In whole blood and plasma, [^{11}C]-3-PHNO showed rapid initial clearance, followed by slower clearance from ~10 minutes following administration.

Biodistribution of [^{11}C]-3-PHNO in the brain

Table 2 presents the temporal profile of ^{11}C radioactivity biodistribution in brain ROIs following [^{11}C]-3-PHNO administration. At the earliest (2 minute) time-point, high levels of radioactivity were detected in all brain regions sampled, indicating rapid uptake to the brain across the blood-brain barrier. By the 10-minute time-point, all brain ROIs except the striatum showed marked radioactivity clearance, whilst the striatum retained high radioactivity levels at all time-points. The temporal profile of striatal radioactivity content is illustrated in Figure 2.

The olfactory bulbs and olfactory tubercles, inferior and superior colliculi and thalamus showed moderate radioactivity content, whilst in the entorhinal cortex, hippocampus and cerebellum radioactivity content was low.

Table 2 also provides the regional [^{11}C]-3-PHNO SBRs relative to the cerebellum. High SBRs were obtained in the striatum, as illustrated in Figure 2. Results also suggested moderate levels of specific binding in the olfactory bulbs, and olfactory tubercles, inferior and superior colliculi, hypothalamus and thalamus during this time period (SBRs >0.5 and

uptake units at both 30 and 60 minutes significantly greater than those in the cerebellum (paired two-tailed t-test, $p>0.05$)). In the entorhinal, prefrontal and somatosensory cortices, hippocampus, and medulla/pons, [^{11}C]-3-PHNO uptake at 30-60 minutes was not consistently higher than that in the cerebellum – in some cases resulting in negative SBR values.

Competition studies

Figure 3 and Table 3 illustrate the effect of pre-treatment with raclopride and PHNO on regional [^{11}C]-3-PHNO activity. With the exception of the entorhinal cortex and hippocampus, pre-treatment with unlabelled PHNO and raclopride produced significant reductions in [^{11}C]-3-PHNO uptake units in all ROIs ($F_{(2,10)} = 6.5$ to 179.6; $p < 0.05$). In the entorhinal cortex and hippocampus, there were similar trends in the data which did not reach defined levels of statistical significance (entorhinal cortex: $F_{(2,10)} = 4.1$; $p = 0.061$; hippocampus: $F_{(2,10)} = 3.9$; $p = 0.066$).

In the above biodistribution study, it was assumed that the cerebellum would exhibit minimal amounts of [^{11}C]-3-PHNO specific binding and therefore be suitable as a reference region for calculation of SBRs. This assumption was proved to be erroneous as [^{11}C]-3-PHNO uptake in the cerebellum was significantly reduced (~29% in both cases) following pre-treatment with either unlabelled PHNO or raclopride (see Table 3, ANOVA: $F_{(2,10)} = 12.871$; $p = 0.003$). The presence of specific binding in the cerebellum infers that regional SBRs calculated using the cerebellum as a reference region, as above, are likely to be underestimated.

Using the uptake unit values obtained at baseline and in the presence of unlabelled PHNO and raclopride, (as presented in Table 3 and Figure 3), it is possible to estimate the non displaceable binding (ND) using graphical analysis assuming steady state conditions (Lassen et al., 1995). Here, (UU1 – UU2) = RO2·UU1 – RO2·ND, where UU1 and UU2 are the uptake units in the baseline and blocking conditions respectively, and RO2 is the receptor occupancy in the blocking condition. When UU1 is plotted against (UU1-UU2), as shown for both the PHNO and raclopride blocking conditions in Figure 4, RO2 is given by the slope and ‘true’ ND by minus intercept/slope. Similar results were obtained under both blocking conditions; for PHNO, the plot is described as $y = 0.9947x – 0.3412$; $R^2 = 0.9952$, and for raclopride $y=0.9997x – 0.3496$; $R^2 = 0.9969$. This analysis demonstrates that unlabelled PHNO and raclopride both produced >99% receptor occupancy, and estimates ND as 0.3410 in the PHNO condition and 0.3506 in the raclopride condition. Regional SBR values estimated using the cerebellar reference region and PHNO and raclopride blocking ND values are given in Table 4. Whilst estimates from PHNO and raclopride blocking data are similar (less than 5% in the striatum), it is clear that SBRs calculated using a cerebellar reference region are markedly underestimated. When [^{11}C]-3-PHNO striatal SBR is calculated from blocking data ND estimates, this value ranges from 5.18 to 5.36 (as estimated from PHNO and raclopride blocking data respectively).

Metabolism

HPLC analysis of rat plasma and brain samples revealed two peaks, as illustrated in the example HPLC chromatograms in Figure 5. The major peak, occurring at around 10 minutes, corresponded to un-metabolized [^{11}C]-3-PHNO. Elution of a smaller, more polar peak, corresponding to a radiolabeled metabolite (M1), occurred at ~4 minutes.

The time-course of the composition of radioactive species in the plasma and brain following injection of [^{11}C]-3-PHNO are presented in Table 5. In plasma, [^{11}C]-3-PHNO was rapidly metabolized and in brain tissue, the radioactivity attributed to the polar metabolite M1 was minimal (3-7%).

Positron emission tomography

When regional [^{11}C]-3-PHNO distribution, measured as uptake units 60 minutes following radiotracer administration, in the 13 brain regions analyzed was compared in non-anesthetized (n=3) and anesthetized (scanned, n=5) control animals a significant positive correlation was detected (linear regression: R^2=0.657; p=0.001), indicating that isoflurane anesthesia did not affect [^{11}C]-3-PHNO brain biodistribution.

Figure 6 illustrates the images that were obtained in the control or amphetamine-treated rats using the quad-HIDAC tomograph system. The reduction in [^{11}C]-3-PHNO ‘SBR’ is clearly seen in the 4mg/kg amphetamine group compared to control. Pre-treatment with 4mg/kg amphetamine produced 53 and 57% reductions in ‘SBR’ in the dorsal and ventral striata respectively. The mean±SD ‘SBR’ in the dorsal striata was 3.21±0.57 in control animals and 1.50±0.06 in amphetamine pre-treated animals. The mean±SD ‘SBR’ in the ventral striata was 2.38±0.45 in control animals and 1.01±0.09 in amphetamine pre-treated animals. These reductions were statistically significant after correction for inequality of variance: dorsal striatum $t_{(5.154)}$ = 7.303; p=0.001); ventral striatum $t_{(5.467)}$=7.230; p=0.001).

Of the extrastriatal regions sampled, amphetamine administration was associated with significant decreases in [^{11}C]-3-PHNO ‘SBR’ in all areas ($t_{(9)}$=2.765 to 4.623; p = 0.021 to 0.001) except the hippocampus ($t_{(9)}$=0.109; ns) and superior colliculus ($t_{(9)}$=0.578; ns) (data not shown). These extrastriatal PET results should be interpreted with caution in the absence of further confirmation, as partial volume, spill-over effects and the presence of specific binding in the cerebellar reference region may bias results.

Discussion

Much of the [^{11}C]-3-PHNO data presented here are consistent with the existing [^{11}C]-(+)-PHNO literature and therefore demonstrate equivalence across research centers and that labeling of PHNO at an alternate molecular position does not markedly alter radiotracer binding profile or pharmacokinetics. Specifically, the profiles of metabolism, brain uptake and regional biodistribution, specific binding and sensitivity to amphetamine of [^{11}C]-3-PHNO were similar to those previously reported for [^{11}C]-(+)-PHNO (Galineau et al., 2006; Ginovart et al., 2006; McCormick et al., 2008; Narendran et al., 2006; Rabiner et al., 2009; Wilson et al., 2005). In extension of previous findings, the present data demonstrate the

presence of [^{11}C]-3-PHNO specific binding in several extrastriatal brain regions, indicating that it may be possible to assess $D_{2/3}$ receptor occupancy outside of the striatum.

[^{11}C]-3-PHNO was rapidly metabolized in the rat and the data indicate that polar metabolites did not readily cross the blood-brain barrier. At the latest time-point measured (60 minutes following [^{11}C]-3-PHNO administration), polar metabolites accounted for 87% of radioactivity in the plasma but only 7% radioactivity in brain tissue. For comparison, in the metabolism study of Wilson et al., (2005), 40 minutes after [^{11}C]-3-PHNO administration 74% activity in plasma and 5% activity in brain tissue was accounted for by polar metabolites. The similarity of these values indicates that [^{11}C]-3-PHNO and [^{11}C]-(+)-PHNO show equivalent metabolism profiles. Although there may be differences in [^{11}C]-3-PHNO and [^{11}C]-(+)-PHNO metabolism between rats and man (Swart et al., 1991; Wilson et al., 2005), these data suggest that that quantification of [^{11}C]-3-PHNO brain uptake and distribution in PET images is unlikely to be confounded by the presence of polar metabolites.

In the periphery, following [^{11}C]-3-PHNO administration, the highest levels of carbon-11 radioactivity accumulation occurred in the lung and kidney, and intermediate values were observed in the spleen, liver, heart, testes and walls of the duodenum, large intestine and stomach. Excretion of [^{11}C]-3-PHNO and/or its metabolites by urinary and fecal elimination was indicated by the high levels of [^{11}C]-3-PHNO that were measured in the urine and content of the small intestine. Although we are not aware of previously published data on [^{11}C]-(+)-PHNO biodistribution, this pattern of peripheral biodistribution is similar to that previously reported for the $D_{2/3}$ agonists [^{11}C]-apomorphine (Zilstra et al., 1993) and [^{11}C]-NPA (Hwang et al., 2000).

[^{11}C]-3-PHNO showed rapid uptake into the brain and a pattern of biodistribution consistent with previous reports of [^{11}C]-(+)-PHNO and [^{3}H]-(+)-PHNO brain biodistribution (Nobrega and Seeman, 1994; Wilson et al., 2005). This biodistribution profile was not affected by isoflurane anesthesia. Consistent with previous findings, the highest levels of [^{11}C]-3-PHNO accumulation occurred in the D_2-rich striatum. The majority of the [^{11}C]-3-PHNO signal in the striatum was due to specific binding at $D_{2/3}$ sites; pre-treatment with 1mg/kg unlabelled PHNO or 2mg/kg raclopride reduced the striatal radioactivity content (uptake units) by approximately 83%. For comparison with previously published data, when calculated as SBR relative to the cerebellum these reductions are in the range of 96%, and ‘true’ SBR values suggest >99% occupancy occurred. Previous studies have reported that similar saturating doses of $D_{2/3}$ antagonists produce >90% reductions in striatal SBR relative to the cerebellum, and are therefore in the same range as data reported here (Galineau et al., 2006; Ginovart et al., 2006; McCormick et al., 2008; Wilson et al., 2005).

A potential limitation of small animal radiotracer binding and PET studies is the amount of receptor occupancy resulting from injection of the radiotracer itself (see Hume et al., 1998). To meet model assumptions, receptor occupancy from radiotracer injection must be minimal. Using the [^{11}C]-(+)-PHNO ED50 of 0.002 mg/kg, derived in cats (see Galineau et al., 2006), the estimated occupancy of $D_{2/3}$ receptors by [^{11}C]-3-PHNO in the current study is 9.80±3.45%. Whilst this degree of occupancy may lead to underestimation of [^{11}C]-3-

PHNO specific binding, there was no significant correlation between the amount of stable PHNO injected and striatal SBR in control animals (df(9), r=0.107; *p*=0.755). In the present study, the range of specific activity injected therefore did not explain variance in SBR estimates. However, as non-negligible levels of occupancy were achieved, this finding highlights the need to control for variation in specific activity in future studies.

PET data in rats confirmed the sensitivity of striatal [^{11}C]-3-PHNO binding to increases in extracellular concentrations of the endogenous agonist DA: administration of 4mg/kg amphetamine i.v. produced a 53% reduction in [^{11}C]-3-PHNO SBR in the striatum, when estimated using the cerebellum as a reference region. These reductions are accordant with previous results for [^{11}C]-(+)-PHNO obtained in rats using *ex vivo* dissection (McCormick et al., 2008; Wilson et al., 2006), and β-microprobes (Galineau et al., 2006) and cats using PET (Ginovart et al., 2006).

Moderate levels of [^{11}C]-3-PHNO uptake were also observed in several extrastriatal regions - most notably in the olfactory bulbs and tubercles, thalamus and hypothalamus and inferior and superior colliculi. In these areas, and also the prefrontal and somatosensory cortices and pons/medulla (which displayed lower levels of [^{11}C]-3-PHNO uptake), [^{11}C]-3-PHNO uptake reflected specific binding to $D_{2/3}$ receptors, as uptake units were significantly reduced by pre-treatment with unlabelled PHNO or raclopride. This pattern of distribution is accordant with that previously reported for [^{3}H]-(+)-PHNO (Nobrega and Seeman, 1994) and $D_{2/3}$ receptor distribution in the rat brain (Bouthenet et al., 1987; Camps et al., 1990; Levant et al., 1993). In select extrastriatal regions, PET data also revealed significant decreases in [^{11}C]-3-PHNO SBR (relative to the cerebellum) following amphetamine administration. Further confirmation of these effects is required, using both *ex vivo* dissection data to avoid partial volume effects and a metabolite corrected plasma input function to avoid the use of a cerebellar reference region. Nonetheless, these preliminary data tentatively indicate that radiolabeled PHNO binding in extrastriatal brain regions may also be sensitive to changes in endogenous dopamine concentrations.

Autoradiographical studies in mice lacking the D_3 receptor demonstrate that the majority of binding of [^{3}H]-(+)-PHNO in extrastriatal regions (hypothalamus, habenula, substantia nigra, ventral pallidum) is attributable to the D3 receptor subtype (Rabiner et al., 2009). Similarly, PET studies in baboons demonstrate a predominance of D_3 receptors in contributing to [^{11}C]-(+)-PHNO binding in the substantia nigra / ventral tegmental area, thalamus and globus pallidus (Narendran et al., 2006; Rabiner et al., 2009). On the basis of this evidence, it is likely that the majority of the thalamic and hypothalamic [^{11}C]-3-PHNO signal observed in the current study is attributable to D_3 receptor binding. In order to confirm this hypothesis and determine the relative contribution of D_2 and D_3 receptor subtypes to [^{11}C]-3-PHNO specific binding observed in other extrastriatal areas, blocking studies with D_2 and D_3 - selective compounds are required. Nonetheless, in extension to the findings of Rabiner et al., (2009), these data suggest that radiolabeled PHNO may be useful in assessing drug occupancy at extrastriatal $D_{2/3}$ receptors.

In the cerebellum, administration of unlabelled PHNO or raclopride also produced marked and significant (29%) reductions in [^{11}C]-3-PHNO signal, suggesting that nearly a third of

the cerebellar [^{11}C]-3-PHNO signal was due to specific binding. This result conflicts with previous rat β-microprobe and cat PET studies which report an absence of [^{11}C]-(+)-PHNO specific binding in the cerebellum (Galineau et al., 2006; Ginovart et al., 2006). In agreement with the present study, autoradiographical studies reveal [^{3}H]-(+)-PHNO specific binding to D_3 receptors in lobules 9 and 10 of the mouse cerebellar cortex and, in baboons, D_3 antagonist administration produces dose-dependent decreases in [^{11}C]-(+)-PHNO binding in the cerebellum as visualized with PET (Rabiner et al., 2009). In the primate study of Rabiner et al., (2009) decreases in [^{11}C]-(+)-PHNO cerebellar binding following D_3 antagonist administration occurred to a maximum of 28%, consistent with the estimated proportion (~29%) of the cerebellar signal attributable to specific binding in the present study. On the basis of the findings of Rabiner et al., (2009) we attribute [^{11}C]-3-PHNO specific binding in the cerebellum to the D3 receptor. Binding to D_3 receptors has similarly been proposed to account for specific binding of the high affinity $D_{2/3}$ radiotracer [^{11}C]-FLB-457 in the cerebellum (Ahmad et al., 2006; Asselin et al., 2007).

These results question the validity of the cerebellum as a reference region in estimation of radiolabelled PHNO specific binding. Our data demonstrates that [^{11}C]-3-PHNO SBRs are underestimated when the cerebellum is assumed to reflect only non displaceable binding: In the striatum an SBR of ~5.3 is obtained using ND estimates from blocking studies, whilst an SBR of only ~4.1 is obtained using cerebellar ND estimates. Use of the cerebellum as a reference tissue may lead to erroneous estimation of regional alterations in $D_{2/3}$ receptor occupancy, produced by either changes in extracellular DA concentrations or administration of pharmacological compounds with $D_{2/3}$ affinity. This applies to the rat PET data presented here relating to change in ‘SBR’ following amphetamine administration. In man, previous kinetic analysis of [^{11}C]-(+)-PHNO revealed data in the cerebellum was better fitted by a two compartment than a one compartment model with 7% of cerebellar radioactivity accounted for by the second compartment (Ginovart et al., 2007). Although other explanations exist, such as kinetic distinction of free and non-specific binding compartments, it is also possible that this second compartment may reflect specific binding to $D_{2/3}$ receptors.

In conclusion, the regional binding profile, specificity and metabolism of [^{11}C]-3-PHNO is similar to that previously reported for [^{11}C]-(+)-PHNO, and the data presented here further supports the use of radiolabeled PHNO in imaging striatal $D_{2/3}$ receptor availability *in vivo*. In addition, the presence of specific binding of [^{11}C]-3-PHNO in several extrastriatal regions indicates that it may also be possible to quantify $D_{2/3}$ receptor occupancy in select brain areas outside the striatum using radiolabeled PHNO. However, as non-negligible levels of [^{11}C]-3-PHNO specific binding also occur in the cerebellum, caution is required when employing this area as a reference region for quantitative analyses.

Acknowledgments

This work was funded by GlaxoSmithKline. We would like to thank Dr Erik Årstad and Dr Edward G Robins (MDX Research, GE Healthcare, Hammersmith Hospital) and Dr Eugenii A Rabiner (GlaxoSmithKline Imaging Centre, Imperial College London) for their valuable input to the work detailed in this manuscript.

References

Ahmad R, Hirani E, Grasby PM, Hume SP. Effect of reduction in endogenous dopamine on extrastriatal binding of [11C]FLB 457 in rat brain-an ex vivo study. Synapse. 2006; 59(3):162–72. [PubMed: 16358331]

Asselin MC, Montgomery AJ, Grasby PM, Hume SP. Quantification of PET studies with the very high-affinity dopamine D2/D3 receptor ligand [11C]FLB 457: re-evaluation of the validity of using a cerebellar reference region. J Cereb Blood Flow Metab. 2007; 27(2):378–392. [PubMed: 16736043]

Brown, DJ.; Luthra, SK.; Brady, F.; Prenant, C.; Dijkstra, D.; Wikstrom, H.; Brooks, D. Labelling of the D2 Agonist (+)-PHNO Using [11C]-Propionyl Chloride. Proceedings of the XIIth International Symposium on Radiopharmaceuical Chemistry; Uppsala, Sweden. 1997; Chichester, U.K.: Wiley; 1997. p. 565-566.

Bouthenet ML, Martres M-P, Sales N, Schwartz J-C. Detailed mapping of dopamine D-2 receptors in rat central nervous system by autoradiography with [125I]iodosulpride. Neuroscience. 1987; 20(1): 117–155. [PubMed: 2882443]

Camps M, Kelly PH, Palacios JM. Autoradiographic localization of dopamine D1 and D2 receptors in the brain of several mammalian species. J Neural Transm Gen Sect. 1990; 80:105–127. [PubMed: 2138461]

Cumming P, Wong DF, Dannals RF, Gillings N, Hilton J, Scheffel U, Gjedde A. The competition between endogenous dopamine and radioligands for specific binding to dopamine receptors. Ann N Y Acad Sci. 2002; 965:440–450. [PubMed: 12105119]

Freedman SB, Patel S, Marwood R, Emms F, Seabrook GR, Knowles MR, McAllister G. Expression and pharmacological characterization of the human D3 dopamine receptor. J Pharmacol Exp Ther. 1994; 268:417–426. [PubMed: 8301582]

Galineau L, Wilson AA, Garcia A, Houle S, Kapur S, Ginovart N. In vivo characterization of the pharmacokinetics and pharmacological properties of [11C]-(+)-PHNO in rats using an intracerebral beta-sensitive system. Synapse. 2006; 60(2):172–83. [PubMed: 16715499]

García-Argüello, SF. Development of dopamine and serotonin agonist radioligands for PET studies [Doctor of Philosophy Thesis]. Imperial College London, University of London; UK: 2007.

Ginovart N, Galineau L, Willeit M, Mizrahi R, Bloomfield PM, Seeman P, Houle S, Kapur S, Wilson AA. Binding characteristics and sensitivity to endogenous dopamine of [11C]-(+)-PHNO, a new agonist radiotracer for imaging the high-affinity state of D2 receptors in vivo using positron emission tomography. J Neurochem. 2006; 97:1089–1103. [PubMed: 16606355]

Ginovart N, Willeit M, Rusjan P, Graff A, Bloomfield PM, Houle S, Kapur S, Wilson AA. Positron emission tomography quantification of [11C]-(+)-PHNO binding in the human brain. J Cereb Blood Flow Metab. 2007; 27:857–871. [PubMed: 17033687]

Graff-Guerrero A, Willeit M, Ginovart N, Mamo D, Mizrahi R, Rusjan P, Vitcu I, Seeman P, Wilson AA, Kapur S. Brain region binding of the D2/3 agonist [11C]-(+)-PHNO and the D2/3 antagonist [11C]raclopride in healthy humans. Hum Brain Mapp. 2008a; 29(4):400–410. [PubMed: 17497628]

Graff-Guerrero A, Mizrahi R, Agid O, Marcon H, Barsoum P, Rusjan P, Wilson AA, Zipursky R, Kapur S. The Dopamine D(2) Receptors in High-Affinity State and D(3) Receptors in Schizophrenia: A Clinical [(11)C]-(+)-PHNO PET Study. Neuropsychopharmacology. 2008b doi: 10.1038/npp.2008.199.

Hirani E, Sharp T, Sprakes M, Grasby P, Hume S. Fenfluramine evokes 5-HT2A receptor-mediated responses but does not displace [11C]MDL 100907: small animal PET and gene expression studies. Synapse. 2003; 50(3):251–60. [PubMed: 14515343]

Houston GC, Hume SP, Hirani E, Goggi JL, Grasby PM. Temporal characterisation of amphetamine-induced dopamine release assessed with [11C]raclopride in anaesthetised rodents. Synapse. 2004; 51(3):206–12. [PubMed: 14666518]

Hume SP, Myers R, Bloomfield P, Opacka-Juffry J, Cremer J, Ahier RG, Luthra SK, Brooks DJ, Lammertsma AA. Quantitation of carbon-11-labeled raclopride in rat striatum using positron emission tomography. Synapse. 1992; 12:47–54. [PubMed: 1411963]

Hume SP, Gunn RN, Jones T. Pharmacological constraints associated with positron emission tomographic scanning of small laboratory animals. Eur J Nucl Med. 1998; 25(2):173–176. [PubMed: 9473266]

Hume S, Hirani E, Opacka-Juffry J, Myers R, Townsend C, Pike V, Grasby P. Effect of 5-HT on binding of [(11)C] WAY 100635 to 5-HT(IA) receptors in rat brain, assessed using in vivo microdialysis and PET after fenfluramine. Synapse. 2001; 41:150–159. [PubMed: 11400181]

Hwang DR, Kegeles LS, Laruelle M. (−)-N-[(11) C]propyl-norapomorphine: a positron-labeled dopamine agonist for PET imaging of D(2) receptors. Nucl. Med. Biol. 2000; 27:533–539. [PubMed: 11056366]

Laruelle M. Imaging synaptic neurotransmission with in vivo binding competition techniques: a critical review. J Cereb Blood Flow Metab. 2000; 20(3):423–451. [PubMed: 10724107]

Lassen NA, Bartenstein PA, Lammertsma AA, Prevett MC, Turton DR, Luthra SK, Osman S, Bloomfield PM, Jones T, Patsalos PN, O'Connell MT, Duncan JS, Andersen JV. Benzodiazepine receptor quantification in vivo in humans using [11C]flumazenil and PET: application of the steady-state principle. J Cereb. Blood Flow Metab. 1995; 15(1):152–165. [PubMed: 7798333]

Levant B, Grigoriadis DE, DeSouza EB. [3H]quinpirole binding to putative D2 and D3 dopamine receptors in rat brain and pituitary gland: a quantitative autoradiographic study. J Pharmacol Exp Ther. 1993; 264(2):991–1001. [PubMed: 8437136]

Madras BK, Fahey MA, Canfield DR, Spealman RD. D1 and D2 dopamine receptors in caudate-putamen of non-human primates (Macaca fascicularis). J. Neurochem. 1988; 51:934–943. [PubMed: 2970527]

McCormick PN, Kapur S, Seeman P, Wilson AA. Dopamine D2 receptor radiotracers [(11)C](+)-PHNO and [(3)H]raclopride are indistinguishably inhibited by D2 agonists and antagonists ex vivo. Nucl Med Biol. 2008; 35:11–17. [PubMed: 18158938]

Myers R, Hume S. Small animal PET. Eur Neuropsychopharmacol. 2002; 12:545–555. [PubMed: 12468017]

Narendran R, Hwang DR, Slifstein M, Talbot PS, Erritzoe D, Huang Y, Cooper TB, Martinez D, Kegeles LS, Abi-Dargham A, Laruelle M. In vivo vulnerability to competition by endogenous dopamine: comparison of the D2 receptor agonist radiotracer (_)-N-[11C]propyl-norapomorphine ([11C]NPA) with the D2 receptor antagonist radiotracer [11C]-raclopride. Synapse. 2004; 52:188–208. [PubMed: 15065219]

Narendran R, Slifstein M, Guillin O, Hwang Y, Hwang DR, Scher E, Reeder S, Rabiner E, Laruelle M. Dopamine (D2/3) receptor agonist positron emission tomography radiotracer [(11)C]-(+)-PHNO is a D(3) receptor preferring agonist in vivo. Synapse. 2006; 60:485–495. [PubMed: 16952157]

Nobrega JN, Seeman P. Dopamine D2 receptors mapped in rat brain with [3H](+)PHNO. Synapse. 1994; 17(3):167–72. [PubMed: 7974199]

Rabiner EA, Slifstein M, Nobrega J, Plisson C, Huiban M, Raymond R, Diwan M, Wilson AA, McCormick P, Gentile G, Gunn RN, Laruelle MA. In vivo quantification of regional dopamine-D3 receptor binding potential of (+)-PHNO: Studies in non-human primates and transgenic mice. Synapse. 2009; 63:782–793. [PubMed: 19489048]

Richfield EK, Penney JB, Young AB. Anatomical and affinity state comparisons between dopamine D1 and D2 receptors in the rat central nervous system. Neuroscience. 1989; 30:767–777. [PubMed: 2528080]

Robb RA. The biomedical imaging resource at Mayo Clinic. IEEE Trans Med Imaging. 2001; 20(9): 854–867. [PubMed: 11585203]

Sautel F, Griffon N, Levesque D, Pilon C, Schwartz JC, Sokoloff P. A functional test identifies dopamine agonists selective for D3 versus D2 receptors. Neuroreport. 1995; 6:329–332. [PubMed: 7756621]

Seeman P, Ulpian C. DopamineD1 andD2 receptor selectivities of agonists and antagonists. Adv. Exp. Med. Biol. 1988; 235:55–63. [PubMed: 2976254]

Seeman P, Ulpian C, Larsen RD, Anderson PS. Dopamine receptors labelled by PHNO. Synapse. 1993; 14:254–262. [PubMed: 7902615]

Seeman P, Tallerico T, Ko F. Dopamine displaces [3H]domperidone from high-affinity sites of the dopamine D2 receptor, but not [3H]raclopride or [3H]spiperone in isotonic medium: Implications for human positron emission tomography. Synapse. 2003; 49(4):209–215. [PubMed: 12827639]

Seeman P, Ko F, Willeit M, McCormick P, Ginovart N. Antiparkinson concentrations of pramipexole and PHNO occupy dopamine D2(high) and D3(high) receptors. Synapse. 2005a; 58:122–128. [PubMed: 16088951]

Seeman P, Weinshenker D, Quirion R, Srivastava LK, Bhardwaj SK, Grandy DK, Premont RT, Sotnikova TD, Boksa P, El-Ghundi M, O'Dowd BF, George SR, Perreault ML, Männistö PT, Robinson S, Palmiter RD, Tallerico T. Dopamine supersensitivity correlates with D2high states, implying many paths to psychosis. Proc Natl Acad Sci USA. 2005b; 102:3513–3518. [PubMed: 15716360]

Seeman P, Schwarz J, Chen JF, Szechtman H, Perreault M, McKnight GS, Roder JC, Quirion R, Boksa P, Srivastava LK, Yanai K, Weinshenker D, Sumiyoshi T. Psychosis pathways converge via D2high dopamine receptors. Synapse. 2006; 60(4):319–346. [PubMed: 16786561]

Seneca N, Finnema SJ, Farde L, Gulyas B, Wikstrom HV, Halldin C, Innis RB. Effect of amphetamine on dopamine D2 receptor binding in nonhuman primate brain: a comparison of the agonist radioligand [11C]MNPA and antagonist [11C]raclopride. Synapse. 2006; 59:260–269. [PubMed: 16416444]

Sibley DR, De Lean A, Creese I. Anterior pituitary dopamine receptors. Demonstration of interconvertible high and low affinity states of the D-2 dopamine receptor. J Biol Chem. 1982; 257:6351–6361. [PubMed: 6176582]

Sokoloff P, Giros B, Martres M-P, Bouthenet M-L, Schwartz J-C. Molecular cloning and characterization of a novel dopamine receptor D3 as a target for neuroleptics. Nature. 1990; 347:146–151. [PubMed: 1975644]

Sokoloff P, Andrieux M, Besancon R, Pilon C, Martres MP, Giros B, Schwartz JC. Pharmacology of human dopamine D3 receptor expressed in a mammalian cell line: Comparison with D2 receptor. Eur J Pharmacol. 1992; 225:331–337. [PubMed: 1354163]

Swart PJ, Jansman FG, Drenth BF, de Zeeuw RA, Dijkstra D, Horn AS. Impact of structural differences on the in vitro glucuronidation kinetics of potentially dopaminergic hydroxy-2-aminotetralins and naphthoxazines using rat and human liver microsomes. Pharmacol. Toxicol. 1991; 68(3):215–219. [PubMed: 1676161]

Willeit M, Ginovart N, Kapur S, Houle S, Hussey D, Seeman P, Wilson AA. High-affinity states of human brain dopamine D2/3 receptors imaged by the agonist [11C]-(+)-PHNO. Biol Psychiatry. 2006; 59:389–394. [PubMed: 16373068]

Willeit M, Ginovart N, Graff A, Rusjan P, Vitcu I, Houle S, Seeman P, Wilson AA, Kapur S. First human evidence of d-amphetamine induced displacement of a D2/3 agonist radioligand: A [11C]-(+)-PHNO positron emission tomography study. Neuropsychopharmacology. 2008; 33(2):279–289. [PubMed: 17406650]

Wilson AA, McCormick P, Kapur S, Willeit M, Garcia A, Hussey D, Houle S, Seeman P, Ginovart N. Radiosynthesis and evaluation of [11C]-(+)-4-propyl-3,4,4a,5,6,10b hexahydro-2H-naphthooxazin-9 -ol as a potential radiotracer for in vivo imaging of the dopamine D2 high-affinity state with positron emission tomography. J Med Chem. 2005; 48:4153–4160. [PubMed: 15943487]

Zijlstra S, van der Worp H, Wiegman T, Visser GM, Korf J, Vaalburg W. Synthesis and in vivo distribution in the rat of a dopamine agonist: ([11C]methyl)norapomorphine. Nucl Med Biol. 1993; 20(1):7–12. [PubMed: 8096418]

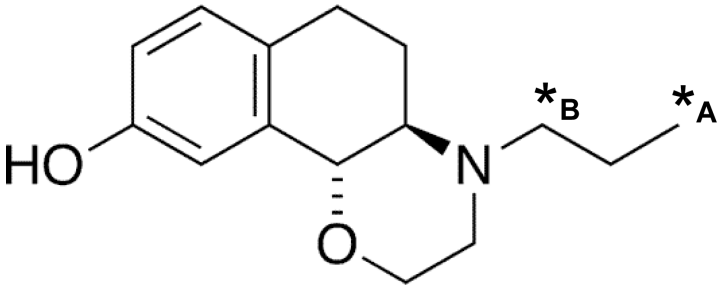

Figure 1.

The structure of PHNO is presented with the alternative ^{11}C-labeling sites indicated by asterisks: *A indicates the labeling position resulting from the novel radiosynthesis route used in the current investigation (García-Argüello, 2007). For comparison, *B indicates the ^{11}C -labeling position resulting from the radiosynthesis route of Wilson et al., (2005), as employed in previously published studies.

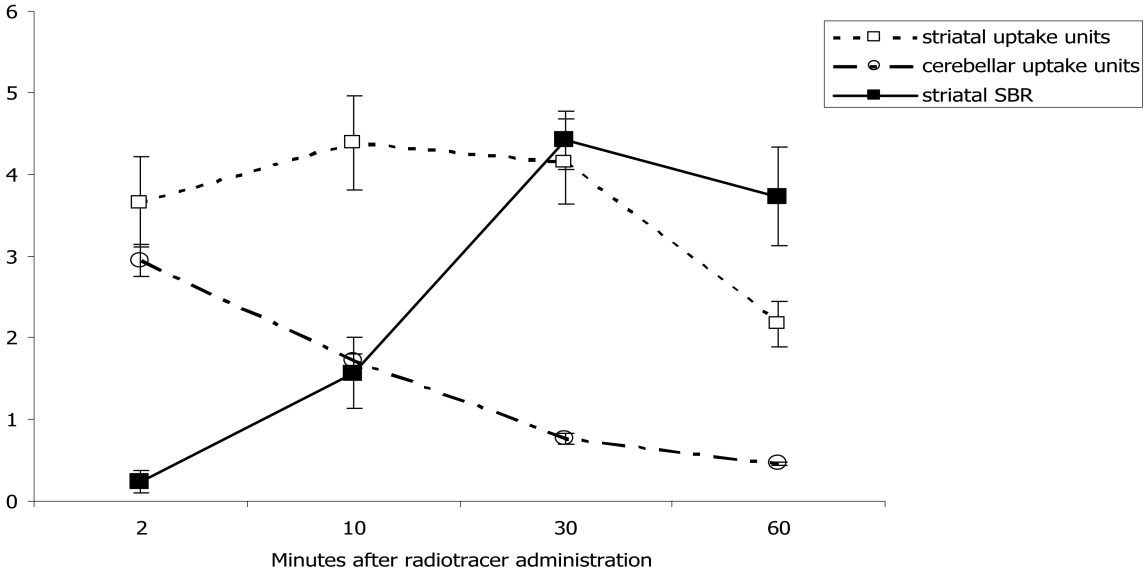

Figure 2.

Time-course of radioactivity content in the striatum after injection of [^{11}C]-3-PHNO. The figure illustrates [^{11}C]-3-PHNO striatal (open squares) and cerebellar (open circles) uptake units (mean±SD) and the striatal to cerebellar 'specific' binding ratios (SBR: (uptake units$_{(ROI)}$ − uptake units$_{(cerebellum)}$)/(uptake units$_{(cerebellum)}$) (filled squares, mean±SD). Striatal and cerebellar radioactivity content was measured 2, 10, 30 and 60 minutes following intravenous administration of ~280μCi [^{11}C]-3-PHNO. Regional radioactivity content was measured in 3 rats at each time-point.

Europe PMC Funders Author Manuscripts

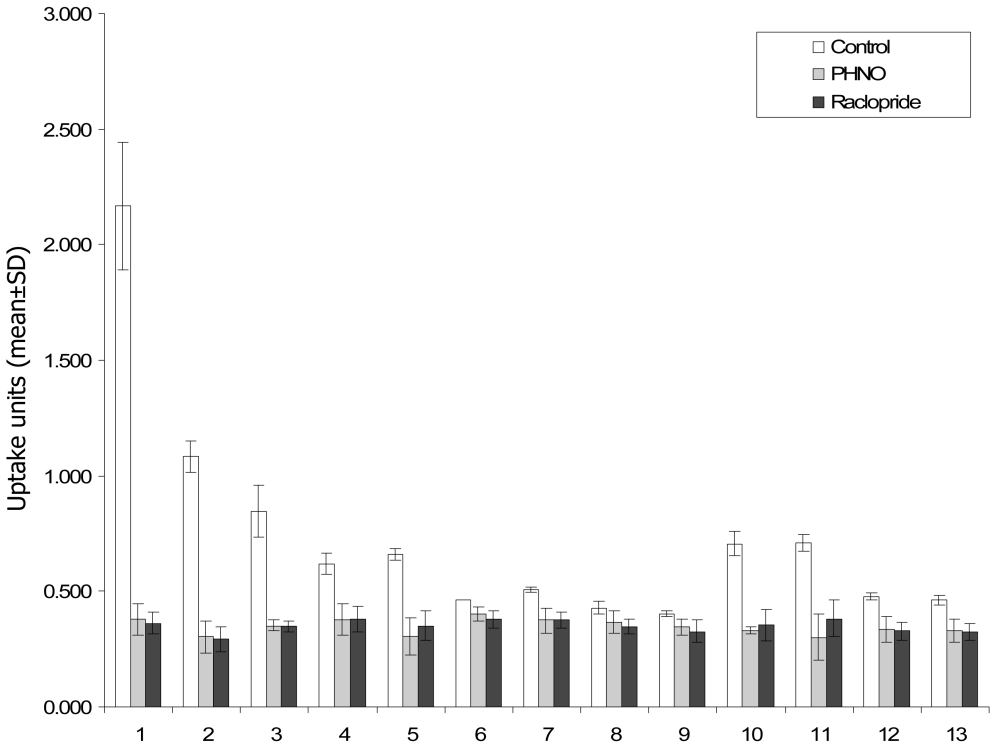

Figure 3.

Biodistribution of [^{11}C]-3-PHNO in control animals (n=3, clear bars) or following pre-treatment with unlabelled PHNO (1mg/kg i.v. n=4, grey bars) or raclopride (2mg/kg i.v.; n=4, black bars). Data is presented as uptake units (mean±SD) and was collected 60 minutes following administration of ~280μCi [^{11}C]-3-PHNO i.v. Brain regions are coded as follows: 1: striata; 2: olfactory bulbs; 3: olfactory tubercles; 4: thalamus; 5: hypothalamus; 6: prefrontal cortex; 7: somatosensory cortex; 8: entorhinal cortex 9: hippocampus; 10: inferior colliculi; 11: superior colliculi; 12: medulla with pons; 13: cerebellum. Pre-treatment with unlabelled PHNO or raclopride significantly reduced ($p<0.05$) [^{11}C]-3-PHNO uptake units in all brain regions except the entorhinal cortex and hippocampus.

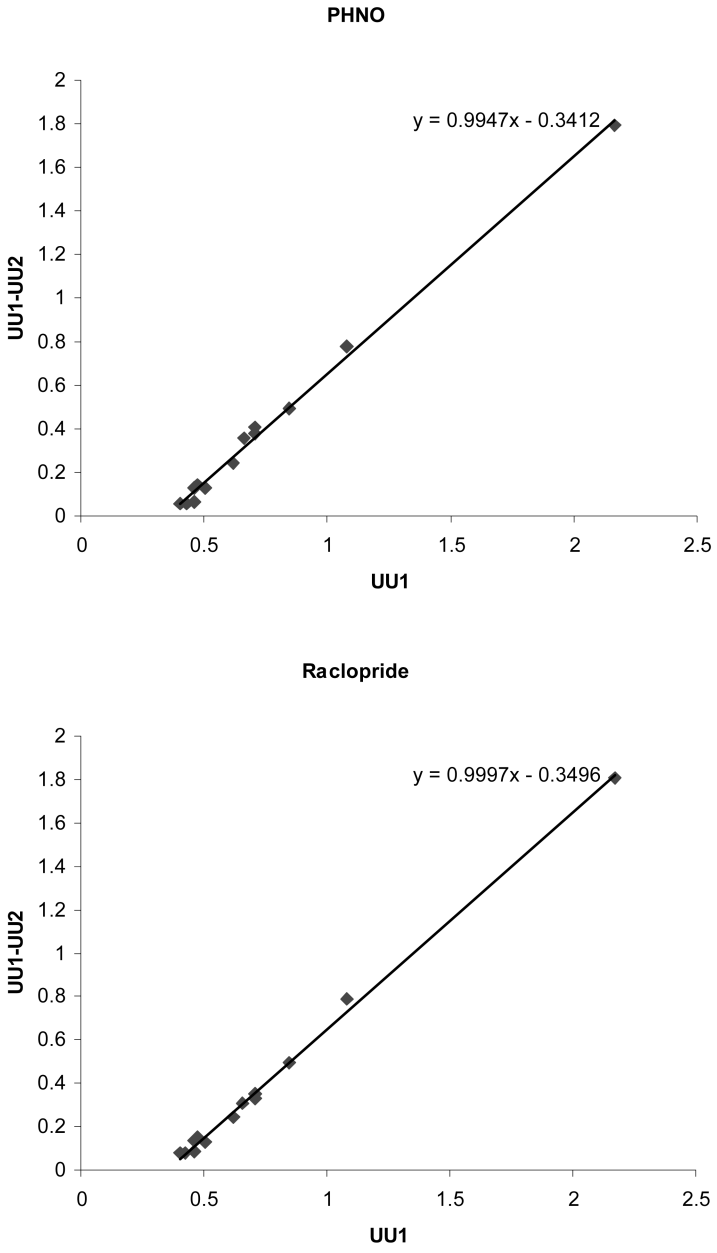

Figure 4.

Graphical analysis of [^{11}C]-3-PHNO data to estimate receptor occupancy and volume of distribution of non-displaceable radiotracer (ND). UU: uptake units at baseline (UU1) and following administration of unlabelled PHNO (UU2, top panel) or raclopride (UU2, bottom panel). Receptor occupancy is given by the slope and ND by the intercept/slope. Under both blocking conditions, occupancy was >99%, whilst ND was estimated at 0.34-0.35.

Europe PMC Funders Author Manuscripts

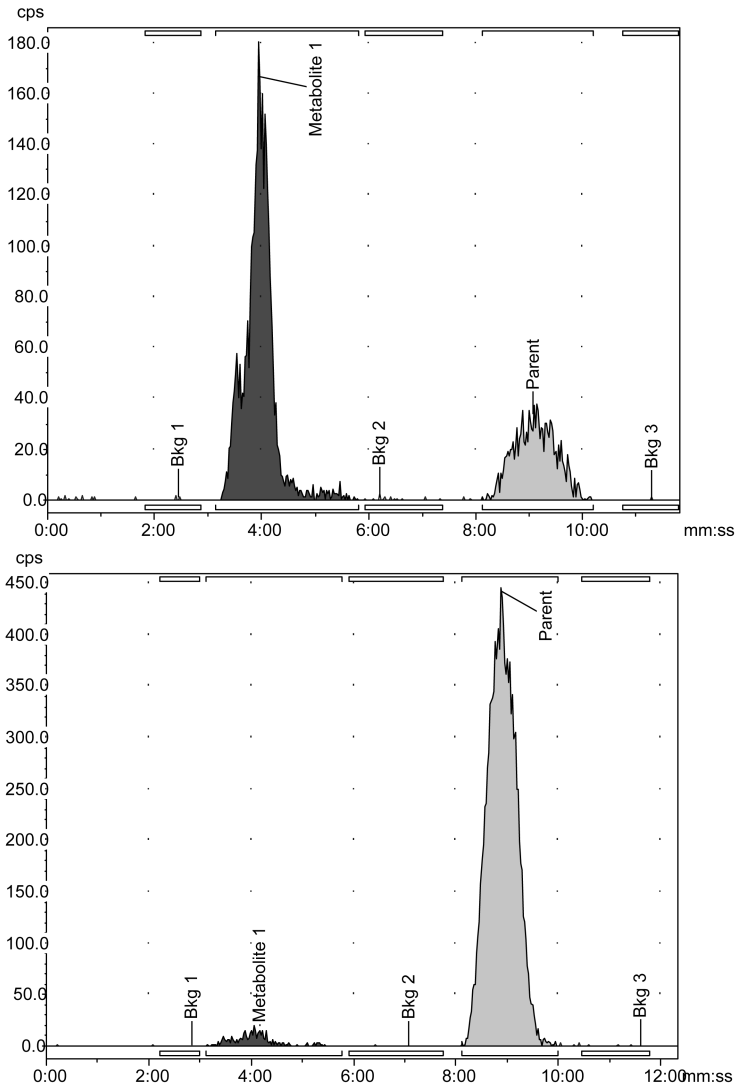

Figure 5.

Sample HPLC chromatograms following injection of [^{11}C]-3-PHNO. Chromatograms are shown for data collected 30 minutes after [^{11}C]-3-PHNO administration in plasma (top) and brain (bottom). The peak visible at ~4 minutes corresponds to polar radiolabeled metabolite (M1), whilst and the peak at ~10 minutes corresponds to unmetabolized parent compound ([^{11}C]-3-PHNO).

Europe PMC Funders Author Manuscripts

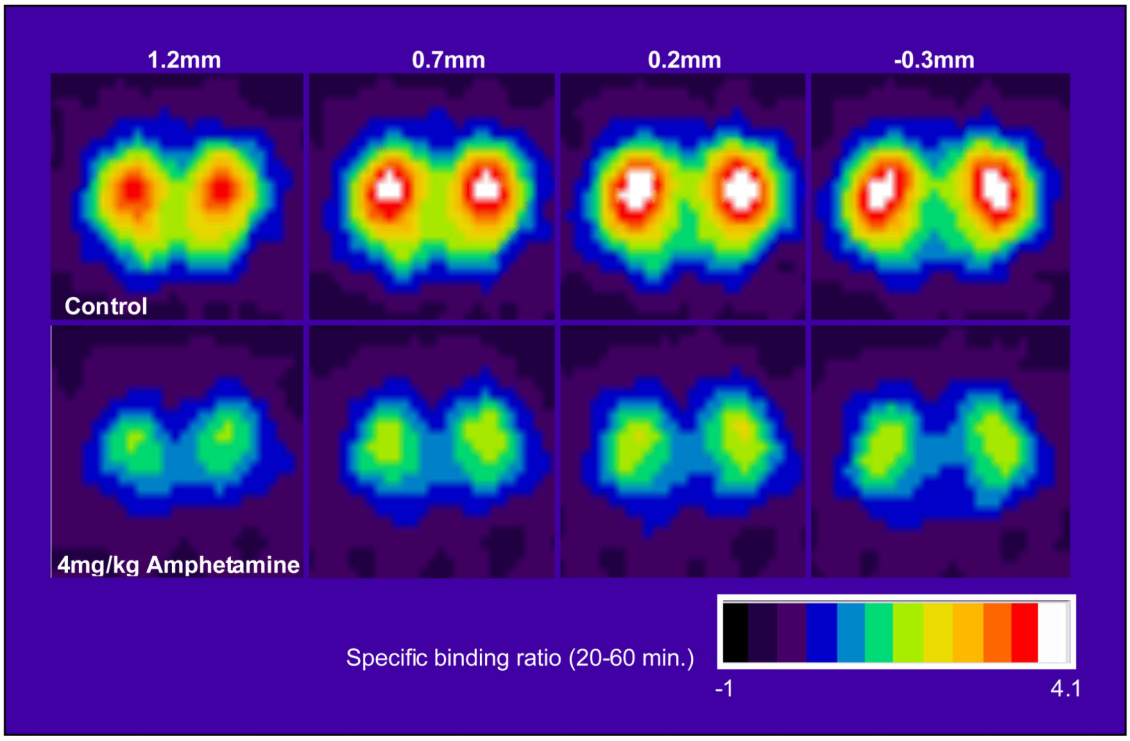

Figure 6.

The images show [^{11}C]-3-PHNO average 'specific' binding ratios (obtained by dividing individual images by sampled cerebellar values) sampled at steady state (20-60 minutes following [^{11}C]-3-PHNO injection) in rats. Four coronal slices at the level of the striatum (with distances from bregma indicated) are presented. The top row presents mean images from control animals (n=6), where the striata are clearly visible as bilateral hotspots. Mean images from animals administered amphetamine (4mg/kg i.p. n=5) are presented in the bottom row. Reductions in [^{11}C]-3-PHNO binding in the striatum in amphetamine-treated compared to control animals are clearly visible.

Europe PMC Funders Author Manuscripts

Table 1

Time-course of ^{11}C radioactivity in peripheral organs and tissues of the rat following [^{11}C]-3-PHNO injection. Awake rats were administered ~280μCi [^{11}C]-3-PHNO i.v. and were euthanized 2, 10, 30 or 60 minutes later (3 rats at each time-point). ^{11}C activity was counted in peripheral organs and tissues and expressed as uptake units (mean ± SD).

Sample	2 min	10 min	30 min	60 min
Heart	2.48±0.23	0.85±0.15	0.51±0.26	0.25±0.00
Lung	9.55±0.96	3.93±1.01	1.62±0.57	1.08±0.10
Liver	2.76±0.47	3.03±0.65	3.13±1.01	1.73±0.21
Kidney	7.69±0.38	2.87±0.10	1.44±0.28	1.05±0.23
Spleen	3.91±0.45	2.38±0.33	0.70±0.16	0.46±0.03
Stomach	1.68±0.45	1.05±0.18	1.36±0.78	0.38±0.15
Small intestine	3.68±1.09	3.36±1.15	4.60±3.96	1.55±1.14
Small intestine content	10.83±5.20	15.54±12.33	11.11±7.71	7.05±2.17
Large intestine	1.97±0.54	0.87±0.12	0.55±0.04	1.12±1.42
Large intestine content	0.18±0.17	0.15±0.11	1.19±1.91	0.11±0.15
Testes	1.07±0.26	1.13±0.08	0.87±0.06	0.47±0.04
Skeletal muscle	0.56±0.12	0.48±0.05	0.3±0.01	0.17±0.02
Fat	0.48±0.33	0.44±0.16	0.62±0.05	0.39±0.04
Skin	0.64±0.21	0.40±0.14	0.40±0.02	0.25±0.06
Urine	0.53±0.23	2.88±15.97	20.27±8.14	16.85±9.18
Whole blood	0.54±0.20	0.40±0.00	0.26±0.08	0.16±0.05
Plasma	0.60±0.12	0.47±0.09	0.29±0.02	0.25±0.00

Table 2

Time-course of ^{11}C radioactivity in brain regions of the rat following [^{11}C]-3-PHNO injection. Awake rats were administered ~280μCi [^{11}C]-3-PHNO i.v. and were euthanized 2, 10, 30 or 60 minutes later (3 rats at each time-point). ^{11}C activity was counted in dissected brain regions and expressed as both mean±SD uptake units and mean±SD 'specific' binding ratio relative to the cerebellum (SBR: (uptake units$_{(ROI)}$ − uptake units$_{(cerebellum)}$)/(uptake units$_{(cerebellum)}$).

Region		2 min	10 min	30 min	60 min
Striatum	*Uptake units*	3.66±0.55	4.38±0.57	4.15±0.52	2.17±0.28
	SBR	0.24±0.14	1.57±.43	4.41±.35	3.73±0.60
Olfactory bulbs	*Uptake units*	3.50±0.41	2.53±0.59	2.07±0.11	1.08±0.06
	SBR	0.19±0.07	0.49±0.40	1.73±0.33	1.36±0.24
Olfactory tubercles	*Uptake units*	3.69±0.56	2.55±0.09	1.42±0.17	0.85±0.11
	SBR	0.25±0.11	0.49±0.09	0.86±0.30	0.84±0.18
Thalamus	*Uptake units*	3.51±0.44	1.45±0.11	1.01±0.14	0.62±0.04
	SBR	0.19±0.07	0.29±0.15	0.31±0.06	0.35±0.08
Hypothalamus	*Uptake units*	3.86±0.61	1.49±0.11	0.97±0.01	0.66±0.02
	SBR	0.31±0.16	0.31±0.02	0.27±0.44	0.44±0.09
Prefrontal cortex	*Uptake units*	3.66±0.37	2.00±0.12	0.82±0.07	0.46±0.00
	SBR	0.24±0.05	0.17±0.01	0.07±0.02	0.01±0.04
Somatosensory cortex	*Uptake units*	3.61±0.20	1.87±0.09	0.89±0.17	0.51±0.01
	SBR	0.23±0.09	0.09±0.03	0.16±0.12	0.10±0.06
Entorhinal cortex	*Uptake units*	3.13±0.50	1.82±0.04	0.72±0.02	0.43±0.03
	SBR	0.06±0.10	0.06±0.03	−0.05±0.09	−0.07±0.04
Hippocampus	*Uptake units*	2.43±0.10	1.74±0.07	0.76±0.07	0.40±0.01
	SBR	−0.17±0.03	0.01±0.03	−0.00±0.00	−0.12±0.02
Medulla with Pons	*Uptake units*	3.34±0.30	2.09±0.07	0.95±0.09	0.48±0.02
	SBR	0.13±0.05	0.22±0.04	0.25±0.04	0.04±0.02
Inferior colliculi	*Uptake units*	5.09±0.64	2.59±0.10	1.17±0.06	0.71±0.05
	SBR	0.72±0.16	0.51±0.11	0.54±0.15	0.54±0.12
Superior colliculi	*Uptake units*	3.69±0.44	2.41±0.29	1.22±0.11	0.71±0.04
	SBR	0.25±0.07	0.41±0.08	0.60±0.08	0.55±0.12
Cerebellum	Uptake units	2.95±0.20	1.72±0.09	0.77±0.07	0.46±0.02

Europe PMC Funders Author Manuscripts

Table 3

Effect of pre-treatment with unlabelled PHNO or raclopride on [^{11}C]-3-PHNO binding. The table presents data from control rats (no pre-treatment; n = 3), and rats administered unlabelled PHNO (1 mg/kg; n = 4), or the D2/3 antagonist raclopride (2 mg/kg; n = 4) i.v. five minutes before [^{11}C]-3-PHNO administration. Data were collected 60 minutes later and are expressed as uptake units (mean±SD). The percentage reduction in uptake units relative to control values is presented and results of one-way analysis of variance (ANOVA) analyses for each ROI are also provided.

	Control	PHNO mean±SD (%)	Raclopride mean±SD (%)	ANOVA $F_{(2,10)}$; p
Striata	2.168±0.28	0.378±0.07 (83%)	0.362±0.05 (83%)	164.1; <0.001
Olfactory bulbs	1.082±0.07	0.302±0.07 (72%)	0.292±0.05 (73%)	179.3; <0.001
Olfactory tubercles	0.846±0.11	0.352±0.02 (58%)	0.348±0.02 (59%)	78.0; <0.001
Thalamus	0.620±0.05	0.377±0.07 (39%)	0.379±0.06 (39%)	18.6; 0.001
Hypothalamus	0.660±0.02	0.302±0.08 (54%)	0.352±0.06 (47%)	30.6; <0.001
Prefrontal cortex	0.461±0.00	0.400±0.03 (13%)	0.378±0.04 (18%)	6.5; 0.021
Somatosensory cortex	0.505±0.01	0.373±0.05 (26%)	0.374±0.04 (26%)	12.3; 0.004
Entorhinal cortex	0.427±0.03	0.367±0.05 (14%)	0.347±0.03 (19%)	4.06; 0.061
Hippocampus	0.402±0.01	0.343±0.04 (15%)	0.326±0.05 (19%)	3.9; 0.066
Medulla with Pons	0.706±0.05	0.330±0.02 (30%)	0.354±0.07 (31%)	12.4; 0.004
Inferior colliculi	0.709±0.04	0.300±0.10 (53%)	0.382±0.08 (50%)	56.2; <0.001
Superior colliculi	0.476±0.02	0.335±0.06 (58%)	0.328±0.04 (46%)	23.9; <0.001
Cerebellum	0.459±0.02	0.327±0.05 (29%)	0.325±0.03 (29%)	12.9; 0.003

Europe PMC Funders Author Manuscripts

Table 4

Regional [^{11}C]-3-PHNO specific binding ratio (SBR) estimates calculated using non-displaceable (ND) estimates from cerebellar uptake units, PHNO blocking data or raclopride blocking data. When BP values are calculated from cerebellar uptake units, SBRs are underestimated due to the presence of specific binding in the cerebellum. SBR estimates obtained via graphical analysis of PHNO and raclopride occupancy data represent 'true' values.

	Calculated specific binding ratio		
	ND estimated from cerebellar uptake units	**ND estimated from PHNO block**	**ND estimated from raclopride block**
Striata	3.723	5.358	5.184
Olfactory bulbs	0.576	2.173	2.086
Olfactory tubercles	0.843	1.481	1.413
Thalamus	0.351	0.818	0.769
Hypothalamus	0.438	0.935	0.883
Prefrontal cortex	0.004	0.352	0.315
Somatosensory cortex	0.100	0.481	0.440
Entorhinal cortex	−0.070	0.252	0.218
Hippocampus	−0.124	0.179	0.147
Medulla with Pons	0.538	1.070	1.014
Inferior colliculi	0.545	1.079	1.022
Superior colliculi	0.037	0.396	0.358
Cerebellum	(0)	0.346	0.309

Europe PMC Funders Author Manuscripts

Table 5

Time-course of composition of radioactive species in plasma and brain. The table presents the percentage of ^{11}C radioactivity occurring as unmetabolized parent compound ([^{11}C]-3-PHNO) or a polar radiolabeled metabolite (M1). Data at each time-point was obtained in a single animal.

	% Metabolite (M1)	% Intact parent compound
Plasma		
2 min	52.18	47.82
10 min	68.27	31.73
20 min	74.55	25.45
30 min	71.40	28.60
60 min	86.99	13.01
Brain		
10 min	3.46	96.54
30 min	3.36	96.64
60 min	6.95	93.05